Structural, microstructural, thermal, and electrical properties of Ni/YSZ cermet materials

Ewa Drożdż-Cieśla · Jan Wyrwa · Jolanta Broś ·
Mieczysław Rękas

Abstract Ceramic–metal composites (cermets) containing 4 mol% yttria-zirconia (4YSZ) and Ni particles as anode materials in solid oxide fuel cells were prepared by two methods. The first method involves nickel oxalate dihydrate precipitation on the 4YSZ powder and decomposition at 360 °C in inert Ar atmosphere. The second method consists of impregnation of the 4YSZ pellets with an aqueous solution of nickel nitrate. The temperature of oxalate decomposition was determined on the basis of TG/DTA experiments. Gaseous products of decomposition were analyzed by mass spectrometry. The structure of the materials was characterized by X-ray diffraction, scanning electron microscopy, porosity studies, and particle size measurements. The thermal expansion coefficient (TEC) was determined by dilathometric method. Electrochemical impedance spectroscopy was used to determine the electrical conductivity. Thus, determined TECs, porosity, and electrical properties were found suitable for anode materials of fuel cells.

Introduction

Solid oxide fuel cells (SOFCs) are an alternative means of energy generation to traditional sources. The traditional

SOFC operates at the range of temperature 800–1000 °C. Current developments are concerned with optimizing anode materials with respect to decreasing operating temperature, increasing the efficiency of electrocatalytic fuel oxidation, and cost reduction. The main requirements for SOFC anode are high electron and ion conductivity in operating temperatures, high catalytic activity in oxidation reaction, chemical stability, and thermal compatibilities with other cell components. The traditional Ni/YSZ anode [1, 2] where electrolyte creates a support, meets the majority of these demands. Recently, an anode supported cell (ASC) has been intensely investigated as a modification of traditional Ni/YSZ anode. In this type of anode, nickel acts as an electron conductor and is the catalyst for anode reaction (breaking hydrogen bonds). The YSZ provides support for the fuel cell and simultaneously acts as an O^{2-} ionic conductor. The anode support must have high degree of porosity (around 40–60%) to supply fuel and remove reaction products. Some authors proposed adding pore-forming particles, such as graphite [3, 4] and carbon nanotubes [4], starch [5, 6] or some polymer [7, 8]. Moreover, proper content of nickel should ensure the continuity of nickel catalytic layers. In the case of traditionally prepared anode (by mixing of metal oxides [2]), the percolation threshold of nickel is about 50 wt%. The main disadvantage of those anodes is the tendency of nickel to agglomerate on the YSZ surface at high temperatures. The main result of this is the breakage of nickel layer continuity, and as an effect, a decrease of electron conductivity and catalytic activity of the anode. The reduction of percolation threshold is an extremely important issue because it can reduce the operating temperature of the cell and decrease the value of thermal expansion coefficient (TEC) of its material. The TEC value informs about the range of thermal shrinking of the material, thus the stability of the cell depends on the adjustment of TEC values of its components.

E. Drożdż-Cieśla (✉) · J. Wyrwa · J. Broś · M. Rękas
Faculty of Materials Science and Ceramics,
AGH University of Science and Technology,
al. A. Mickiewicza 30, 30-059 Krakow, Poland
e-mail: eciesla@agh.edu.pl

According to Simwonis et al. [9], the electrical conductivity of the anode depends on the anode microstructure (volume fractions, particle, and pore sizes). Hence, the idea that changing the method of Ni/YSZ material preparation has an effect on the microstructure, thermal properties and related electrical properties, of the cermet materials. In the literature, various methods have been described: impregnation [10], citrate–nitrate combustion synthesis [11], precipitation with buffer solution of $NH_{3(aq)}$ and NH_4HCO_3 [12], co-precipitation method [13], or precipitation of nickel salt on YSZ powder [8]. In this article, two methods of preparation of cermet anode material are compared: "oxalate" and impregnation method. Impregnation is a classical method but in this article the materials are obtained in two different variants of impregnation. The "oxalate" method is interesting as a new method which leads to uniform dispersion of the component metallic and oxide particles on a nanometer scale. Oxalate salts are often used to obtain oxides [14–18]. Nickel oxalate, in contrast to the most d-electron metal salts, decomposes to metallic nickel instead of nickel oxide in inert atmosphere [19]. The results of measurements concerning the structure, microstructure, thermal, and electrical properties of the Ni/YSZ anode material testify to the usefulness of the oxalate and impregnation method.

Experimental

Preparation of materials

4 mol% yttria-zirconia (4YSZ) powder was prepared via co-precipitation of hydrous zirconia gel using an aqueous solution of zirconium(IV) oxychloride octahydrate (Beijing Chemicals Import & Export Corporation) and yttrium(III) nitrite and aqueous ammonia (analytical grade) as a precipitating agent. Y_2O_3 (99.99 %) was dissolved in HNO_3 to prepare the yttrium(III) nitrite solution. Each precursor solution was analytically verified (by classical precipitation method). The co-precipitated gel was washed with distilled water and additionally with ethanol. The powder was then calcined at 700 °C for 1.5 h and after cooling, attrition milled for 2 h.

8YSZ crystallized in a regular structure. This form of ZrO_2 is mechanically worse than the tetragonal form. 4YSZ was prepared in order to obtain mechanically stable tetragonal structure.

The two methods of preparation Ni/YSZ cermet materials are compared. The first is "oxalate" method (M I), the second is impregnation method (M II).

Method I (M I)

The aqueous solution of oxalic acid was mixed with 4YSZ (4 mol% Y_2O_3/ZrO_2) powders at room temperature, then the nickel(II) nitrate solution was added in small portions to the mixture. The suspension was stirred, filtered, washed with distilled water, and dried to constant weight at 80 °C in air. Then, the powder was decomposed for 0.5 h at 360 °C in inert Ar atmosphere (<2 ppm O_2 and <3 ppm H_2O). The temperature of decomposition was selected on the basis of TG/DTA curves and mass spectra analysis (Fig. 1). A heating rate of 2 °C/min was used. The anode materials containing 30, 40, and 50 wt% Ni in the mixture with YSZ were manufactured in this way. After decomposition, disk pellets of 10 mm in diameter and mass about 0.4 g were pressed under 200 MPa.

Method II (M II)

The saturated solution of nickel nitrate was prepared. The disk pellet with porous 4YSZ (like in the M I) was pressed. Next, a solution of nickel nitrate was introduced to the YSZ support either by capillary forces or under 100 kPa pressure. After saturation, disk pallets were dried in 240 °C and calcinated at 800 °C in 10%H_2/90%Ar mixture. The drying temperature was determined from TG/DTA curves of decomposition nickel nitrate in air atmosphere presented by Elmasary et al. [19]. According to Elmasary, 240 °C is a sufficient temperature for complete decomposition of nickel
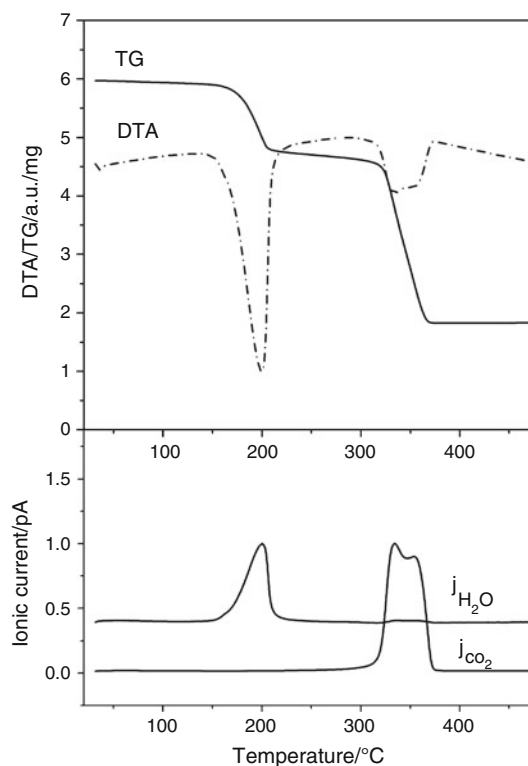

Fig. 1 Thermogravimetric and mass spectrometry results of decomposition nickel oxalate in helium atmosphere. Heating rate $\beta = 2$ °C min^{-1}, platinum crucibles

nitrate. The samples were impregnated with nitrate several times up to nickel amount exceeding 35 wt%. In this way, the sample with the Ni content about 35–42 wt% was obtained.

The pallets obtained in the bath methods (M I and M II) were consolidated at 800 °C for 3 h in a mixture of 10%H_2/Ar.

Apparatus

The phase composition of the powders was determined by X-ray diffraction (XRD) analysis using $Cu_{K\alpha}$ radiation within 2Θ range 20–90° with Philips X'Pert Pro diffractometer.

The scanning electron microscopy (SEM) observations were done using JROL 5400 scanning electron microscope with EDS analyzer.

The measurements of particle size distribution were carried out with Mastersizer 2000 from Malvern Instruments. The measurements of open pore size distribution were performed with PoreMaster 60 from Quantachrome Instruments. The open porosity was calculated on the base of water saturation method. The total porosity was determined by relative geometrical density measurements assuming that densities of metallic Ni and 3YSZ are, respectively: 8.908 and 6.06 g/cm^3.

Temperature of oxalate decomposition was determined from TG/DTA measurements performed on SDT 2960 TA Instruments apparatus. Gaseous products of decomposition were analyzed by a mass spectrometer (Balzers, ThermoStar QMD 300), connected online to SDT apparatus. Values of TEC measurements were carried out with a measuring instrument and "size changing" transducer provided by a DIL 402 C equipment from NETZSCH. Cuboidal samples of a dimension of $2 \times 2 \times 9$ mm^3 were used in the experiments. The measurements were done in the Ar atmosphere containing 5% H_2; a rate of temperature change was 5 °C/min within the temperature range of 20–800 °C. The values of TEC were calculated using the linear regression approximation.

The measurements of electric properties were carried out by electron impedance spectroscopy (EIS) with Solatron SI 1260 Impedance/Gain-Phase Analyzer with the SI 1296 dielectric interface in the temperature range 20–700°C at the frequencies from 0.1 to 10^6 Hz. A flowing gas atmosphere of 10% H_2 in Ar was used.

Results and discussions

Characteristics of 4YSZ support

X-ray analysis of the 4YSZ support showed that the YSZ powder consisted only of tetragonal (94.5 ± 0.5%) and monoclinic (5.5 ± 0.5%) polymorph (Fig. 2). The
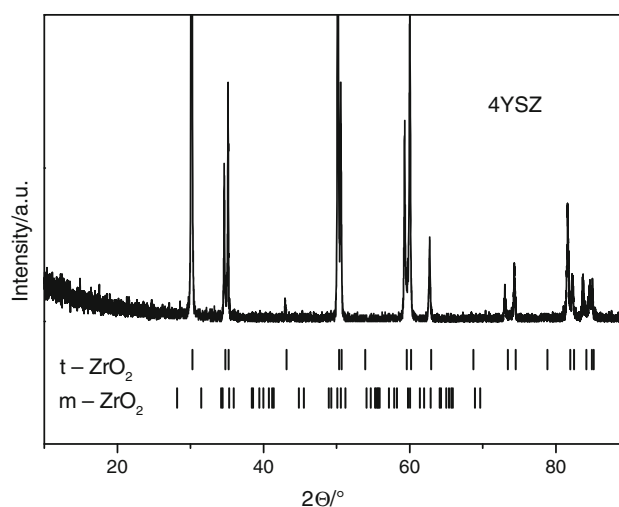

Fig. 2 X-ray diffraction pattern of 4YSZ powder

crystallite size determined from the tetragonal ZrO$_2$ (101) peak broadening was 12.5 ± 0.5 nm. The nanoparticles of YSZ create agglomerates. The results of particle size distribution measurements (Fig. 3) indicate that 90% of the particles are up to 2.55 μm in size. The total porosity calculated from the geometrical density was 64 ± 1%.

Selection of calcination conditions

The nickel oxalate dihydrate in inert atmosphere decomposes in the two stages (Fig. 1), the first is dehydration in the range 180–220 °C and the second is a decomposition of anhydrous oxalate in the range 320–370 °C. The mass losses calculated with TG curves: 18.8 ± 0.4% for dehydration and 47.9 ± 0.5% for decomposition correspond to dehydration of nickel oxalate dihydrate to anhydrous nickel oxalate and subsequent decomposition to metallic nickel.
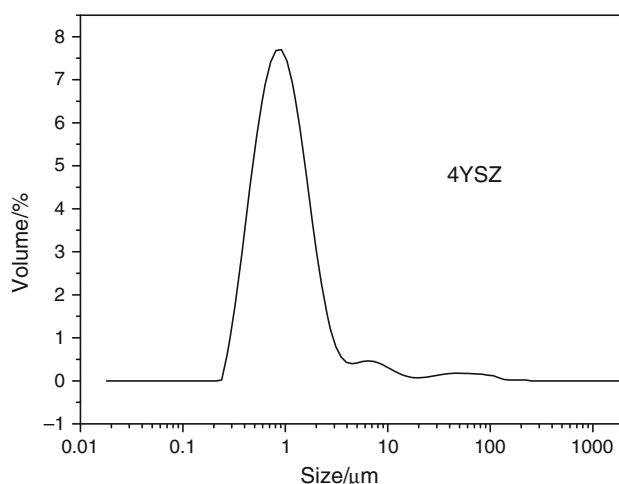

Fig. 3 Particle size distributions of 4YSZ

Table 1 Comparison of open porosity and values of TEC for samples obtained by M I and M II methods

Sample	4 YSZ	Ni/YSZ M I	M II capillary	M II under pressure
Open porosity (%)	64.0 ± 0.8	68.2 ± 1.0	64.0 ± 0.8[a]	64.0 ± 0.8[a]
TEC (K^{-1})	9.84 ± 0.14 × 10^{-6}	9.57 ± 0.14 × 10^{-6} for 40%Ni/4YSZ	–	9.96 ± 0.13 × 10^{-6} for 39.9%Ni/4YSZ

[a] Porosity of YSZ before impregnation

Fig. 4 SEM images of:
a 30%Ni/4YSZ with M I;
b 33.3%Ni/4YSZ M II
capillary; **c** 39%Ni/4YSZ M II
under pressure; **d** cross-section
of 39%Ni/4YSZ M II under
pressure; **e** EDS spectrum for
pointed area with cross-section
of 39%Ni/4YSZ M II under
pressure
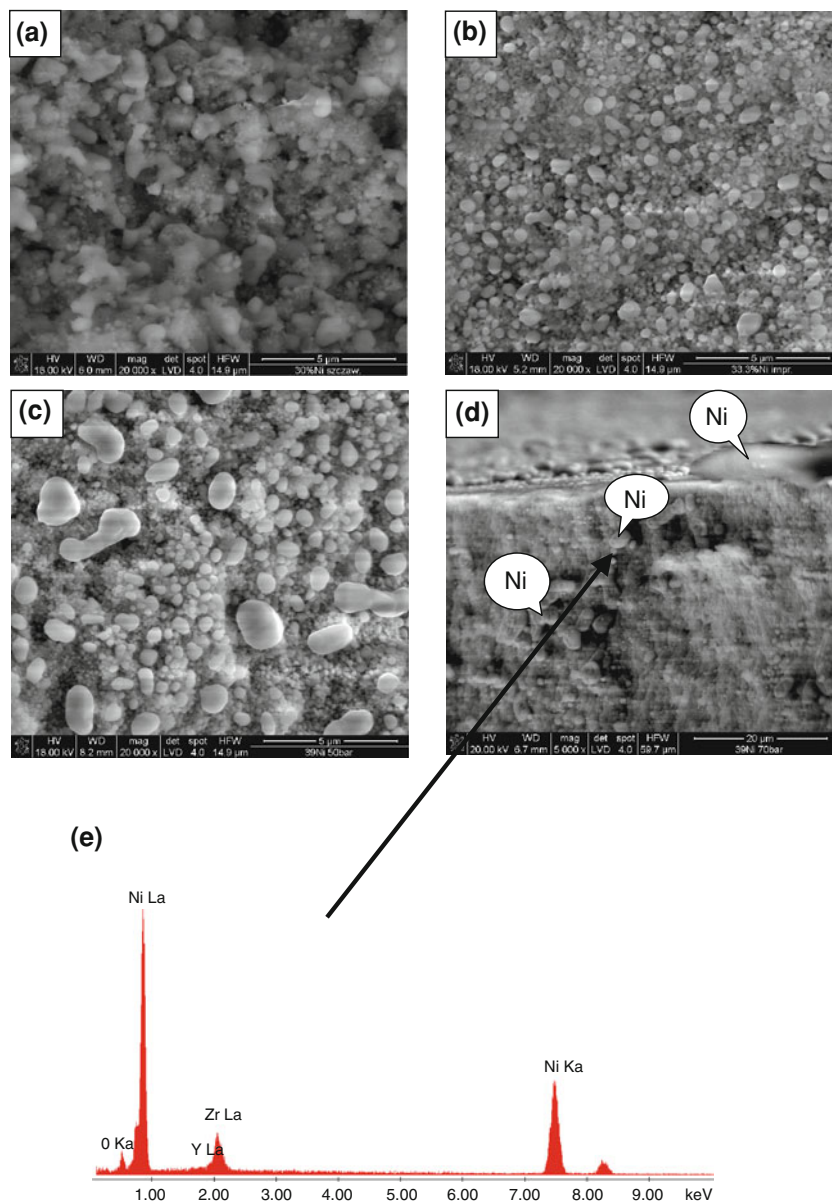
Moreover, analysis of gaseous products (mass spectra analysis) evolving during decomposition confirms water liberation in the first stage and water and carbon dioxide evolving in the second stage.

On the basis of TG/DTA and MS curves, the temperature of nickel oxalate decomposition and heating rate of sample in argon were selected.

Characteristic of cermets

The results of porosity measurement show (Table 1) that in the case of cermets obtained by M I total porosity increased (in comparison with 4YSZ) to 68 ± 1%. The porosity measurements have not been done for the sample synthesized by M II but the pores had to decrease as the result of
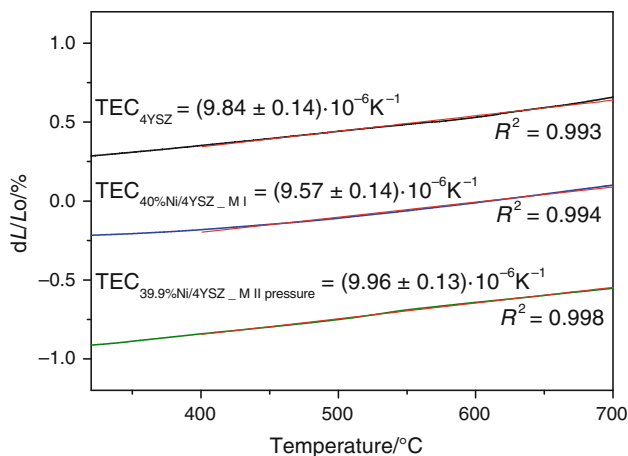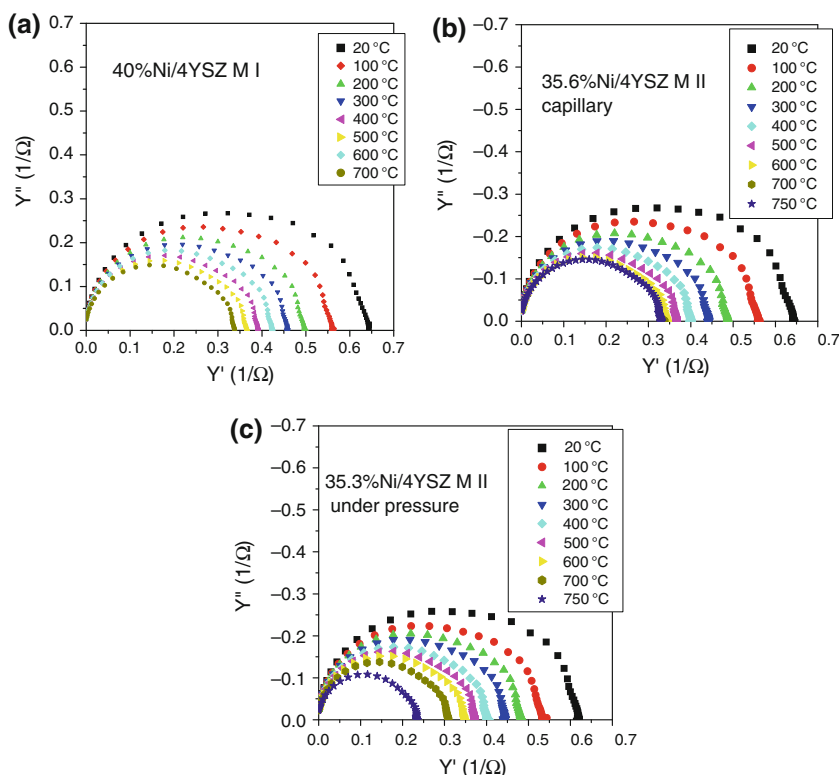
Fig. 5 Dilatometric plots of the 4YSZ and Ni/4YSZ materials. The values of TEC were calculated for range 400–700 °C

Table 2 The composition of the samples which was testified by EIS measurements

Method	M I	M II capillary	M II under pressure
Composition, Ni wt%	30%Ni/4YSZ	33.8%Ni/4YSZ	35.3%Ni/4YSZ
	40%Ni/4YSZ	35%Ni/4YSZ	37.8%Ni/4YSZ
	50%Ni/4YSZ	35.2%Ni/4YSZ	39.9%Ni/4YSZ
		35.6%Ni/4YSZ	40.5%Ni/4YSZ

impregnation. However, even these presented values testified that obtained cermet materials are suitable for SOFC anode. This porosity has been reached by using preparation methods without application of any pore-forming agents.

SEM micrographs (Fig. 4) show that all samples were composed of nano-grains. It was found that cermets obtained by M I and by M II capillary (Fig. 4a, b) were much more homogenous than cermet synthesized by M II under pressure (Fig. 4c). In the case of materials synthesized by M I and M II capillary, the YSZ and nickel grains could not be distinguished. The material obtained by the M I was identified as the most homogenous. In Fig. 4c (opposite to the (a) and (b)), bigger grains of metallic nickel are visible. Figure 4d shows a cross-section of the same pellet (M II under pressure). Larger grains corresponding with metallic nickel are noticeable both in the middle of pallet and on its border. There is an EDS spectrum in Fig. 4e which originated from the pointed area in the middle of the pallet.

TEC was determined on the basis of the length change versus temperature curves (Fig. 5). Dilathometric studies were carried out for support material and for cermets obtained using "oxalate" and impregnation methods. The TEC values calculated for the range of temperature 400–700 °C for the all materials are presented in the Table 1. In this temperature range, there is linearity of the length change versus temperature dependences. Moreover, this range is more interesting than the lower temperature
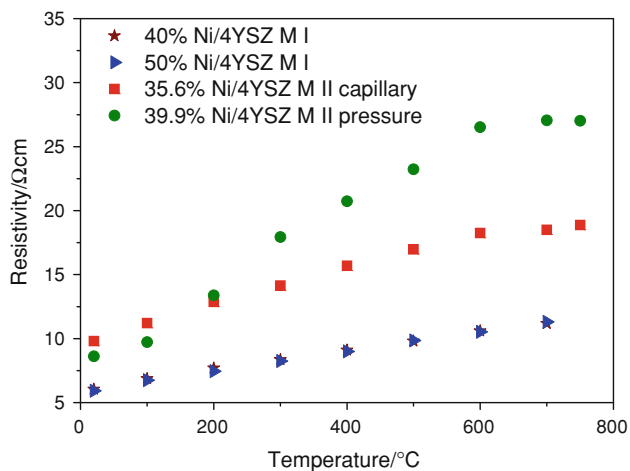
Fig. 6 The experimental Nyquist plots for samples: **a** 40%Ni/YSZ M I; **b** 35.6%Ni/YSZ M II capillary; **c** 35.3%Ni/YSZ M II pressure

Fig. 7 Resistivity of the Ni/YSZ cermets versus temperature determined in the 10%H_2/Ar atmosphere
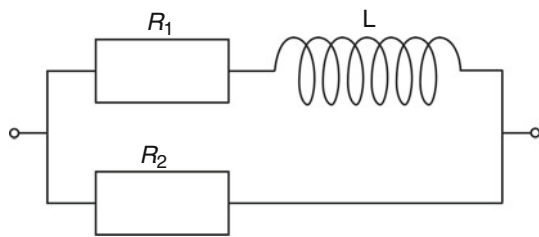

Fig. 8 Equivalent circuits used for interpretation of the impedance spectra (conducting sample with M I)

one with regard to working temperatures of the Ni/YSZ cermet anode. The theoretical TEC values for pure nickel and for fully dense 3YSZ are 17.0×10^{-6} K^{-1} and 10.5×10^{-6} K^{-1}, respectively.

The value of TEC for porous 4YSZ is close to this value for nonporous material. However, the most important finding is that TEC values for obtained cermet materials are close to the TEC value of YSZ. It can indicate a potentially good adjustment between two phases: anode and electrolyte materials. In the consequence, it can prevent cracking of the cell during operation.

The dependence of resistivity of samples versus temperature was determined using impedance spectroscopy measurements in reducing (10%H_2/Ar) atmosphere. The compositions of the samples testified by EIS are shown in Table 2. On the basis of general dependence—the electrical conductivity of metals decreases with increasing temperature—compositions of cermets were chosen in which materials behave as metals (underline in the Table 2). The experimental Nyquist plots for exemplary samples with methods M I and M II are shown, respectively, in Fig. 6a–c. The dependence of resistivity of the samples versus temperature is shown in the Fig. 7. An analysis of the impedance spectra revealed that the equivalent circuits (EC) in Fig. 8

well represent the impedance data for electron conducting samples obtained by M I and M II, respectively. The values of electrical parameters for the sample M I were: ρ_1 in the range 8–15 Ω cm, ρ_2 in the range 580–760 Ω cm and $L = (2.28 \pm 0.02)$ μH. For the sample with M II capillary and under pressure values of specific resistance are, respectively: 1.6–3 Ω cm and 1.6–3.3 Ω cm. Values of R_2 were not measurable. Values of inductance were around 2.20 ± 0.03 μH for both samples. The element R_1-L (Fig. 8) can be attributed to nickel paths. The element R_2 represents the support (zirconia) resistivity in the cermet. The samples in the Table 2 which are not underlined do not reveal metallic character. The EC for them consists of resistance and capacity. The lack of inductor element shows that in those materials nickel does not form conductivity paths.

Conclusions

The two methods of preparation of Ni/4YSZ cermet materials: the "oxalate" and the impregnation method, were compared. Both methods lead to the formation of nanomaterials (XRD and SEM measurements), however, in the case of impregnation under pressure method bigger grains are also visible. The open porosity is significantly larger than the 50% required for SOFC materials.

The values of TECs for samples with M I as with M II are close to value for pure 4YSZ as well. It testifies to a very good thermal compatibility between cermet and YSZ material.

Electrical properties measurements allowed demonstration that the presented method cermet materials synthesis leads to a value of conductivity suitable for SOFC anodes.

The most important fact is that, even below 40 wt% of nickel, it is possible to obtain the conductivity path by proper nickel spreading on the YSZ surface. It is a significant improvement over a traditional anode. Both method presented herein can lead to a decrease in the operating temperature of the cell.

References

1. Badwal SPS, Foger K. Solid oxide electrolyte fuel cell review. Ceram Int. 1996;22:257–65.

2. Minh NQ, Takahashi K. Science and technology of ceramic fuel cells. California: Elsevier; 1995. p. 147–9.
3. Clemmer RMC, Corbin SF. Effect of graphite pore-forming agents on the sintering characteristics of Ni/YSZ composites for solid oxide fuel cell applications. Int J Appl Ceram Technol. www.onlinelibrary.wiley.com/doi/10.1111/j.1744-7402.2011.02639.x/full. Accessed 27 April 2011.
4. Arico E, Tabuti F, Fonseca FC, de Florio DZ, Ferlauto AS. Carbotherml reduction of YSZ-NiO solide oxide fuel cell anode precursor by carbon-based materials. J Therm Anal Calorim. 2009;97:157–61.
5. Savigant SB, Chiron M, Barthet C. Tape casting of new electrolyte and anode materials for SOFCs operated at intermediate temperature. J Eur Ceram Soc. 2007;27(2–3):673–8.
6. Kan H, Lee H. Enhanced stability of Ni-Fe/GDC solid oxide fuel cell anodes for dry methane fuel. Catal Commun. 2010;12:36–9.
7. Lee JH, Heo JW, Lee DS, Kim J, Lee HW, Song HS, Moon JH. The impact of anode mirostructure on the power generating characteristics of SOFC. Solid State Ion. 2003;158:225–32.
8. Kim SD, Moon H, Hyuan SH, Moon J, Kim J, Lee HW. Ni-YSZ cermet anode fabricated from NiO-YSZ composite powder for high-performance and durability of solid oxide fuel cells. Solid State Ion. 2007;178:1304–9.
9. Simwonis D, Tietz F, Stöver D. Nickel coarsening in annealed Ni/8YSZ anode substrates for solid oxide fuel cells. Solid State Ion. 2000;132:241–51.
10. Haberko K, Jasiński M, Pasierb P, Radecka M, Rękas M. Structural and electrical properties of Ni-YSZ cermet materials. J Power Sources. 2010;195:5527–55338.
11. Marinsek M, Zupan K. Microstructure evaluation of sintered combustion-derived fine powder NiO-YSZ. Ceram Int. 2010;36:1075–82.
12. Ying L, Yusheng S, Jianghong G, Yunfa Ch, Zhongtai Z. Preparation of Ni/YSZ materials for SOFC anodes by buffer-solution method. Mater Sci Eng. 2001;86:119–22.
13. Sato K, Ohara S. Synthesis of NiO/YSZ nanocomposite particles using co-precipitation method. Trans JWR. 2009;38(1):85–8.
14. Caballero A, Cruz M, Hernan L, Melero M, Morales J, Rodriguez-Castelon E. Nanocrystalline materials obtained by using a simple, rapid method for rechargeable lithium batteries. J Power Sources. 2005;150:192–201.
15. Drożdż-Cieśla E, Małecki A, Jajko B. Mechanism of thermal decomposition of zirconyl oxalate $ZrOC_2O_4$. J Therm Anal Calorim. 2008;92:939–44.
16. Dollimore D. Thermal decomposition of oxalates. A review. Thermochim Acta. 1987;117:331–63.
17. Dumitru R, Carp O, Budrugeac P, Niculescu M, Segal E. Non-isothermal decomposition kinetics of $[CoC_2O_4 \cdot 2.5H_2O]_n$. J Therm Anal Calorim. 2011;103:591–6.
18. Rejitha KS, Mathew S. Thermoanalytical investigations of tris(ethylenediamine)nickel(II) oxalate and sulphate complexes. J Therm Anal Calorim. 2010;102:931–9.
19. Elmasary MAA, Gaber A, Khater EMH. Thermal decomposition of Ni(II) and Fe(III) nitrates and their mixture. J Therm Anal. 1998;52:489–95.